Thermodynamics of Specific and Nonspecific DNA Binding by Two DNA-Binding Domains Conjugated to Fluorescent Probes

Martin Thompson and Neal W. Woodbury
Department of Chemistry and Biochemistry, Arizona State University, Tempe, Arizona 85287-1604 USA

ABSTRACT The complexes designed in this work combine the sequence-specific binding properties of helix-turn-helix DNA-binding motifs with intercalating cyanine dyes. Thermodynamics of the Hin recombinase and Tc3 transposase DNA-binding domains with and without the conjugated dyes were studied by fluorescence techniques to determine the contributions to specific and nonspecific binding in terms of the polyelectrolyte and hydrophobic effects. The roles of the electrostatic interactions in binding to the cognate and noncognate sequences indicate that nonspecific binding is more sensitive to changes in salt concentration, whereas the change in the heat capacity shows a greater sensitivity to temperature for the sequence-specific complexes in each case. The conjugated dyes affect the Hin DNA-binding domain by acting to anchor a short stretch of amino acids at the N-terminal end into the minor groove. In contrast, the N-terminal end of the Tc3 DNA-binding domain is bound in a well-ordered fashion to the DNA even in the absence of the conjugated dye. The conjugated dye and the DNA-binding domain portions of each conjugate bind noncooperatively to the DNA. The characteristic thermodynamic parameters of specific and nonspecific DNA binding by each of the DNA-binding domains and their respective conjugates are presented.

INTRODUCTION

The design and synthesis of novel sequence-specific DNA-binding agents has attracted considerable interest (Brown and Harding, 1994; Dwyer et al., 1992; Sardesai and Barton, 1997) and has led to a greater understanding of the subtle factors that confer recognition of DNA sequences at the molecular level. Several groups have focused their attention on combining the effects of two different types of binding motifs in the same molecule to develop systems with enhanced selectivity, stronger binding affinity, or that act as a chemical probe or reporter group (Bourdouxhe et al., 1992; Mack and Dervan, 1990; Tokuda et al., 1993). The complexes designed in this work combine the sequence-specific binding properties of HTH DNA-binding motifs with intercalating cyanine dyes. Such conjugates are very attractive as probes of both sequence-dependent thermodynamics and of searching dynamics involved in peptides locating binding sites on DNA. Because the intercalating dyes used in this study fluoresce only when intercalated in DNA, the conjugates only produce measurable signals when bound. This makes it possible to perform very sensitive studies of fluorescence changes due to binding and movement, particularly at the single molecule level, where background fluorescence becomes a very serious issue (Daniel et al., 2000).

Previous studies of a similar system using a zinc finger-intercalating dye conjugate have shown that the properties of the native DNA-binding domain are retained in the conjugate and that the dye acts as a sensitive reporting group of the binding behavior of the oligopeptide (Thompson and Woodbury, 2000a). Here, two new peptide/dye conjugates are described and characterized in terms of the detailed thermodynamic parameters associated with specific and nonspecific binding interactions. In subsequent investigations, these conjugates will be used primarily in fluorescence energy transfer experiments to study the properties of fluorescence resonance energy transfer between intercalated donors and acceptors in DNA, to map out the sequence-dependent potential surface of native DNA binding regions using energy transfer as a distance ruler, and to observe the single-molecule dynamics of linear searching and sequence-specific binding. This future work is critically dependent on a detailed understanding of the thermodynamic parameters that control binding of these conjugates to specific and nonspecific sequences. Because it is necessary to distinguish between effects resulting from protein–DNA interactions and those due to the attached probe, this study compares the unconjugated native DNA-binding domains with the dye-conjugated peptide.

The overall affinity of protein–DNA interactions is determined by the free energy difference between the free and bound forms of each component. The enthalpy and entropy changes for many DNA-binding proteins have opposing effects on the free energy of complex formation. The extent to which the DNA binding of a given protein will be enthalpically or entropically driven is a function of solution conditions, such as temperature, salt concentration, pH, etc. An accepted notion is that sequence-specific interactions between the functional groups on the protein and the binding site on the DNA stabilize the complex by contributing to

Received for publication 22 January 2001 and in final form 15 May 2001.

Abbreviations used: HTH, helix-turn-helix; dsDNA, double stranded deoxyribonucleic acid; Hin, Hin recombinase DNA-binding domain; Tc3, Tc3 transposase DNA-binding domain; TOTc3, thiazole orange-Tc3 transposase DNA-binding domain conjugate; YOHin, oxazole yellow-Hin recombinase DNA-binding domain conjugate;

Address reprint requests to Neal W. Woodbury, Professor of Chemistry and Biochemistry, Arizona State University, Tempe, AZ 85287-1604. Tel. 480-965-3294; Fax: 480-965-2747; E-mail: NWoodbury@asu.edu.

0006-3495/01/09/1793/12 $2.00

the enthalpy component (ΔH). The entropic contribution to the binding free energy, in contrast, has been shown to drive both sequence-specific and nonspecific binding (Bulsink et al., 1985; Takeda et al., 1992). The large positive change in entropy (ΔS), which seems contrary to formation of a higher order complex, is partially derived from the net release of ions and water molecules from the complementary macromolecular surfaces upon protein–DNA association. Studies using DNA sequences ranging from specific to nonspecific show large variations in the enthalpic and entropic contributions (Frank et al., 1997; Oda et al., 1998) for a given protein, suggesting that the energetics of the DNA surface is, to some extent, unique to the protein–DNA interface formed upon binding.

The thermodynamics of many DNA-binding proteins have been studied, but relatively few of the DNA-binding domains themselves have been investigated in great detail aside from conjugated complexes engineered to chemically (Mack and Dervan, 1990; Shin et al., 1991) or photochemically (Sardesai and Barton, 1997; Thompson and Woodbury, 2000b) cleave DNA. The study of individual domains can lead to valuable insights into protein design. Knowing how individual segments work in isolation creates opportunities to mix and match domains to generate new functions or to position nonnative functions into diverse areas.

In this study, the HTH motifs from Hin recombinase and Tc3 transposase, with and without the conjugated intercalating cyanine dyes, are studied by fluorescence anisotropy and relative fluorescence yield. Previous studies using peptide–probe conjugates (Dervan et al., 1984; Sardesai and Barton, 1997; Sluka et al., 1987) show that they retain the ability to recognize the native consensus sequence. This system conjugates a fluorescent intercalating probe to the DNA-binding domain for sensitive studies of the binding properties, as has been shown previously (Thompson and Woodbury, 2000b). The Hin and Tc3 DNA-binding domains are similar in structure and mode of sequence-specific DNA interaction. Both of these DNA-binding domains also have a short length of their C- and N-termini that stabilize binding by forming specific interactions in the minor groove. The HTH motif common to both gets its name from a region of high secondary structure similarity, consisting of a recognition helix, which spans the major groove and exhibits the majority of sequence-specific contacts. A second helix stabilizes the folded structure by forming a hydrophobic pocket and often confers some additional binding stabilization. The HTH motif is found in a wide range of proteins, such as homeodomains (Pabo and Sauer, 1992) and transcription factors (Latchman, 1990; Pabo and Lewis, 1982). These motifs recognize a wide range of short DNA sequences, often with submicromolar binding constants (Bruist et al., 1987). Despite the important role played by HTH-containing proteins in gene expression and repression, no comprehensive study of the thermodynamic parameters of the isolated HTH DNA-binding motif's association with DNA has been performed.

Tc3 of *Caenorhabditis elegans* is a member of the Tc1/*mariner* family of transposable elements. Transposable elements (transposons) are small stretches of DNA that can move from one position in the genome to another (Plasterk, 1996). The enzyme responsible for excision and insertion of the transposon into the genome, called a transposase, is encoded by the transposon sequence. In this particular family of transposons, only a single protein, the transposase, is encoded by the Tc3A gene and is capable of performing the entire transposition reaction in vitro (Lampe et al., 1996; Vos et al., 1996). Crystal structure data (van Pouderoyen et al., 1997) of the HTH motif shows that the N-terminal end of the 52-residue fragment comprising the DNA-binding domain of Tc3 transposase is oriented in the minor groove. This further stabilizes the binding interaction by acting as a "thumb" to grip the DNA. Currently, there is no thermodynamic or binding information for the DNA-binding domain of this protein to complement the crystal structure data.

The other DNA-binding domain used in these studies was derived from the Hin recombinase of *Salmonella typhimurium*, which belongs to the class of DNA-cleaving enzymes known as invertases or recombinases. Hin catalyzes a DNA inversion reaction of a 1-kb segment of the chromosome to control alternate expression of two flagellin genes by switching the orientation of the promoter (Hughes et al., 1992). The Hin proteins recognize and bind to left (*hixL*) and right (*hixR*) sites that flank the invertible segment. A specific DNA–protein complex is formed by the Hin recombinase dimers in the presence of a recombinational enhancer sequence and Fis proteins, which interact directly with the enhancer element. This higher order complex is necessary for strand exchange at the *hix* sites because, after recombination, DNA supercoils are lost, providing energy for the reaction. Crystal structure data of the HTH motif of the Hin protein shows that the N- and C-terminal ends of the 52-residue fragment comprising the DNA-binding domain of Hin recombinase are oriented in the minor groove (Feng et al., 1994). The critical sequence-specific contacts between the Hin monomer and a *hix* half-site are an AT base pair that the protein contacts in both the major and minor groove. This facilitates opening of the DNA duplex, exposing bases to solvent.

The use of solid phase synthesis (SPS) to make these DNA-binding domains facilitates the addition of a fluorophore to a defined location on the peptide, in this case enabling the intercalation of the dye into the double-stranded DNA. In this paper, the thermodynamic parameters for the specific and nonspecific binding of the Hin and Tc3 domains, with and without a conjugated intercalating dye, to DNA are determined.

202 253
TOTc3: N-[TO]-PRGSALSDTERAQLDVMKLLNVSLHEMSRKISRSRHCIRVYLKDPVSYGTS-C

139 190
YOHin: N-[YO]-GRPRAINKHEQEQISRLLEKGHPRQQLAIIFGIGVSTLYRYFPASSIKKRMN-C

FIGURE 1 The primary structure of the TOTc3 and the YOHin conjugates. The 52-amino-acid Tc3 DNA-binding domain tethered to the dye was derived from residues 202–253 of the native Tc3 transposase, and the 52-amino-acid Hin DNA-binding domain tethered to the dye was derived from residues 139–190 of the native Hin recombinase. The location of the appropriate cyanine dye is shown in brackets. The underlined residues are those having α-helical secondary structure.

MATERIALS AND METHODS

Materials

Lepidine, 5-bromovaleric acid, 3-methylbenzothiazole-2-thione, 2-mercaptobenzoxazole, para-methyltoluenesulfonate, iodomethane, anhydrous ethanol, and triethylamine were purchased from Aldrich (Milwaukee, WI) and used without further purification. F-moc amino acids and peptide synthesis reagents were purchased from Advanced Chemtech (Oklahoma City, OK). The F-moc-Lys (Mtt)-OH was purchased from Anaspec (San Jose, CA).

Instrumentation

Peptides were synthesized on a 9050 peptide synthesizer (Millipore, Bedford, MA). Purification of synthetic peptides was performed using high performance liquid chromatography. Absorbance measurements were made on a Cary V spectrophotometer (Varian Instruments, Palo Alto, CA). Steady-state fluorescence and fluorescence anisotropy measurements were performed on a Spex Fluorimeter (Jobin Yvon Inc., Edison, NJ).

Labeled and nonlabeled peptide synthesis, purification and characterization

The cyanine dyes coupled to the DNA-binding domains were synthesized as described previously (Rye et al., 1992; Thompson and Woodbury, 2000b). Labeled and unlabeled peptides were synthesized on PAL-PEG-PS resin by automated solid-phase peptide synthesis using F-moc chemistry (Kent, 1988). For labeled peptides, the carboxylic acid derivative of the cyanine dye is attached by standard O-(7-azabenzotriazol-1-yl)-*N,N,N′,N′*-tetramethyluronium hexafluorophosphate (HATU) coupling chemistry at a selectively deprotected lysine. This procedure was described in a previous publication (Thompson and Woodbury, 2000b).

The peptides were purified by reverse phase high performance liquid chromatography on a Zorbax C_8 column (9.4 mm × 25 cm) (Agilent Tech., Palo Alto, CA) using a water (0.1% TFA)-acetonitrile (0.1% TFA) gradient. Identities of the peptides were confirmed by amino acid analysis and matrix-assisted laser desorption ionization–time of flight mass spectrometry. Stock solution concentrations of both the nonlabeled and labeled peptide were determined spectrophotometrically. The extinction coefficient ϵ_{280nm} = 4200 M^{-1} cm^{-1} calculated for tyrosine absorption (Cantor and Schimmel, 1980) was used for nonlabeled peptides. For the dye-labeled peptides, concentrations were determined from the extinction coefficients of ϵ_{280nm} = 40,500 M^{-1} cm^{-1} for YOHin and ϵ_{280nm} = 50,800 M^{-1} cm^{-1} for TOTc3 (Thompson, 2000). The amino acid sequences of the Tc3 transposase DNA binding domain and the Hin recombinase DNA binding domain are shown in Fig. 1.

DNA synthesis and purification

All oligonucleotides were synthesized on a DNA synthesizer using phosphoramidite chemistry (Caruthers et al., 1987) and purified on a 15% denaturing polyacrylamide gel. Bands were cut out and recovered by soaking the crushed gel pieces in 100 mM Tris, (pH 8.0) 100 mM NaCl buffer for 4–6 h. Extractions were combined and the urea and salts removed by spin filtration or a Sephadex G-15 size exclusion column (Aldrich). Concentrations for purified single-stranded oligonucleotides were calculated using the nearest neighbor method (Fritsch and Maniatus), 1989; Kendrew and Lawrence, 1994) except for the tetramethylrhodamine-labeled strands, which were determined spectrophotometrically by using ϵ_{542nm} = 81,000 M^{-1} cm^{-1} (Haugland, 1996). Nonlabeled strands for use with reverse titrations of the conjugates were annealed using the same molar equivalent of each oligonucleotide. Each tetramethylrhodamine-labeled oligo was annealed with 1.5 molar equivalents of its unlabeled complement. The excess single-stranded DNA is not expected to alter the results because monomeric cyanine dyes do not bind the single-stranded DNA. The oligonucleotides used in this study are shown in Fig. 2.

Fluorescence measurements

Steady-state fluorescence anisotropy and total fluorescence measurements were performed as forward and reverse titrations, respectively, as described previously (Thompson and Woodbury, 2000b). Forward titrations of the tetramethylrhodamine-labeled DNA with nonlabeled DNA-binding domains were performed using 10 nM tetramethylrhodamine-labeled DNA and varying the concentration of the peptide. Vertically polarized excitation at 542 nm was used with detection in the vertical and horizontal planes at 582 nm. Reverse titrations using 1 nM of the appropriate peptide/dye conjugate were performed by varying the concentration of nonlabeled DNA. Excitation was at 480 nm and emission detection at 510 nm for oxazole yellow and 510 and 535 nm, respectively, for thiazole orange samples. Steady-state fluorescence measurements were carried out in 20

TC3: 5'-GCTGACTGCGTTCTATAGGACCCCCCCGCTGACTGCATCA-3'

hixL: 5'-TCTAGATGGCCACGTTATCAAAAACACTATGTCGCACGGC-3'

NS: 5'-TCCATGCACGTCGACGTACGGTCGTACGTCGCACGGCTAC-3'

FIGURE 2 The three 40-base oligonucleotide sequences used in these studies. The native consensus sequences for the Tc3 and the Hin hixL are underlined. A nonspecific sequence that contains neither consensus sequence (NS) is also shown. 5′-Tetramethylrhodamine-labeled oligos identical to these were used for the anisotropy measurements of the nonlabeled DNA-binding domains (see Materials and Methods).

mM Tris (pH 7.6), 150 mM NaCl except in the case of the salt titrations, where the concentration of NaCl is as indicated in the figures and tables. Salt-dependence studies were performed by addition of an appropriate amount of 1 M NaCl in the same Tris buffer to yield the indicated final salt concentration. Temperature-dependence studies were performed by incubating each sample for 30 min at the given temperature. The temperature of the sample was held constant by pumping water through the cuvette holder from a Neslab General Purpose bath (Portsmouth, NH) fit with a flow-through cooler. Each titration was performed at least three times.

Determination of thermodynamic functions

The contribution of the hydrophobic effect and the polyelectrolyte effect to the stability of the conjugate or DNA-binding domain–DNA complex was determined by analyzing the temperature and salt-concentration dependence of the observed association equilibrium constant K_{obs}. For binding to a specific DNA sequence, K_{obs} is given by

$$K_{obs} = \frac{[PD]_{eq}}{[P]_{eq}[D]_{eq}}, \quad (1)$$

where, $[P]_{eq}$ is the concentration of the conjugate or DNA-binding domain, $[D]_{eq}$ is the concentration of DNA, and $[PD]_{eq}$ is the concentration of bound complex at equilibrium. This analysis is based on the assumption that sequence-specific binding can be described as a two-state system. Here, the stability of the bound complex is determined by the differences in the noncovalent interactions between the peptide and the DNA as salt concentration and temperature are varied. Equilibrium titration data were evaluated by fitting to Eq. 1 using a nonlinear least-squares algorithm as previously described (Thompson and Woodbury, 2000b).

Titration data for the interaction of the DNA-binding domains (DBDs) and the conjugated probes with nonspecific DNA are analyzed in terms of the McGhee–von Hippel model for binding to a chain polymer in the absence of any cooperative interactions between ligands (McGhee and von Hippel, 1974):

$$\frac{v}{[L]} = K(1 - nv)\left(\frac{1 - nv}{1 - (n-1)v}\right)^{n-1}, \quad (2)$$

where v is the ratio of bound DBD or probe per DNA base pair, $[L]$ is the free ligand concentration (dye-labeled or nonlabeled HTH), K (M^{-1}) is the intrinsic binding constant for binding by the ligand to a site consisting of n base pairs. It is this intrinsic equilibrium-binding constant, K, that is used in the analyses that follow for nonspecific binding.

Each equilibrium-binding constant value reported is the average of at least three independent titrations. The experimental error in determining equilibrium binding constant values is $\sim\pm 15\%$.

RESULTS

Characterization of the conjugates

The purified 52-amino-acid TOTc3 conjugate was characterized using matrix-assisted laser desorption ionization-time of flight mass spectrometry. The expected mass of TOTc3 is 6209.8 and a sharp peak in its mass spectrum is observed for the singly charged species at (m/e) = 6210.9. By comparison, the expected mass of the Tc3 DNA-binding domain itself is 5843.8 and a sharp peak in its spectrum is observed for the singly charged species at (m/e) = 5841.0. The expected mass of the purified 52-amino-acid YOHin conjugate is 6522.3 and a sharp peak in its mass spectrum is observed for the singly charged species at (m/e) = 6523.8. By comparison, the expected mass of the Hin DNA-binding domain itself is 6163.2 and a sharp peak in its spectrum is observed for the singly charged species at (m/e) = 6160.9. The conjugate was further characterized by reversed phase HPLC. An HPLC analysis of purified conjugates and unlabeled peptides shows only one peak in the chromatograph (data not shown), which confirms the purity of these preparations.

Specific binding by the nonlabeled peptides

The specific binding affinity of the synthetic peptides comprising the Hin and Tc3 domains (sequence shown in Fig. 1) was determined initially without any dye molecules conjugated to the peptides. In each case, this was accomplished by monitoring the anisotropy of a tetramethylrhodamine-labeled dsDNA fragment containing the appropriate binding site (sequences given in Fig. 2) as a function of the concentration of the DNA binding domain being considered. Figure 3 shows representative binding curves at a few selected temperatures and salt concentrations for the association of Hin (Fig. 3 *A*) and Tc3 (Fig. 3 *B*) domains to their respective specific binding sites. The binding constants (K_{obs}) and the corresponding binding free energies (ΔG^0) determined for a more complete series of salt concentrations (0.15–0.25 M Na^+) and temperatures (275–313 K) are shown in Table 1.

Previous studies have shown that the binding constants for both sequence-specific and nonspecific interactions of proteins with DNA are typically strongly dependent on salt concentration in the physiological range in the absence of competitive divalent cations (Revzin, 1990). In Table 1, the equilibrium constant decreases monotonically approximately fourfold when the salt concentration is increased from 0.15 to 0.25 M for both of the two DNA-binding domains studied. In contrast, the dependence of the observed equilibrium constant with temperature is not monotonic. Instead, an increase in binding strength is apparent as the temperature is increased from 275 K to near 300 K for both the Hin and Tc3 binding domains, followed by a decrease in the binding strength as the temperature continues to increase above ~300 K (Table 1). This is due to an unfavorable binding enthalpy at lower temperature that becomes favorable at higher temperature, as described in more detail below.

Specific binding by the dye-labeled peptides (conjugates)

The site-specific DNA binding affinity of the Hin and Tc3 domains was also determined. In this case, the total fluorescence intensity could be used to monitor binding because the conjugated dyes only fluoresce significantly when intercalated into DNA (the fluorescence quantum

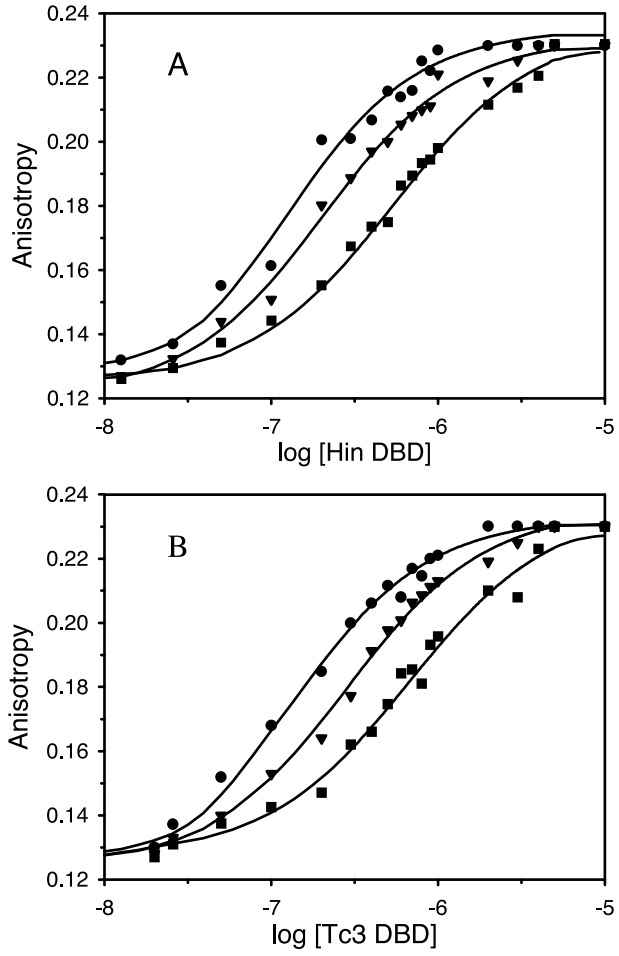

FIGURE 3 Representative binding curves for (*A*) Hin and (*B*) Tc3 binding to their respective tetramethylrhodamine-labeled consensus DNA sequences (Fig. 2). The fluorescence anisotropy of 10-nM tetramethylrhodamine-labeled DNA is plotted as a function of the log of the nonlabeled (*A*) Hin or (*B*) Tc3 concentration at several salt concentrations and temperatures: ●, 298 K, 0.150 M Na^+; ▼, 313 K, 0.150 M Na^+; ■, and 298 K, 0.250 M Na^+. The solid lines represent the best fit to a binding curve.

yield upon intercalation is enhanced ~1000–5000-fold over that in solution). For these binding titrations, monitoring fluorescence intensity is preferable to monitoring fluorescence anisotropy, because energy transfer between the bound intercalating dye and the label on the DNA used in the anisotropy measurements interferes with the experimental determination of the anisotropy. In addition, the measurement of total fluorescence can be generally performed with higher sensitivity than anisotropy measurements, because it does not depend on determining a small difference between the parallel and perpendicular fluorescence readings.

Figure 4 shows representative binding curves determined for the YOHin- and TOTc3-domain conjugates as a function of the concentration of the native consensus sequence for the YOHin (Fig. 4 *A*) or TOTc3 (Fig. 4 *B*) conjugate, respectively. The binding constants (K_{obs}) and

TABLE 1 The equilibrium constants (K_{obs}) and binding free energies determined for sequence-specific binding of Hin and Tc3 with their respective consensus DNA-binding sequences

	Hin recombinase DBD			Tc3 transposase DBD		
Temp (K)	$[Na^+]$ (M)	K_{obs} (M^{-1}) $\times 10^{-6}$	ΔG° (kcal/mol)	$[Na^+]$ (M)	K_{obs} (M^{-1}) $\times 10^{-6}$	ΔG° (kcal/mol)
275	0.150	4.4	−8.4	0.150	7.7	−8.7
278	0.150	8.4	−8.8	0.150	8.6	−8.8
283	0.150	8.6	−9.0	0.150	8.0	−8.9
288	0.150	10.6	−9.3	0.150	13.3	−9.4
293	0.150	10.8	−9.4	0.150	13.2	−9.5
298	0.150	11.1	−9.6	0.150	11.6	−9.6
303	0.150	9.1	−9.7	0.150	14.3	−9.9
308	0.150	6.1	−9.6	0.150	9.8	−9.9
313	0.150	6.1	−9.7	0.150	5.7	−9.7
298	0.175	6.9	−9.3	0.175	11.8	−9.6
298	0.200	4.0	−9.0	0.200	6.4	−9.3
298	0.225	2.5	−8.7	0.225	4.8	−9.1
298	0.250	2.5	−8.7	0.250	3.2	−8.9

the corresponding binding free energies (ΔG^0) determined in this way are given in Table 2 for salt concentrations between 0.15 and 0.25 M Na^+ and temperatures between 275 and 313 K. The equilibrium constant decreases 6- and 14-fold for YOHin and TOTc3, respectively, when the salt concentration is increased from 0.15 to 0.25 M. As was observed for the unconjugated DNA-binding domains, the temperature dependence of the equilibrium-binding constant goes through a maximum in the 295–300 K range (Table 2).

DNA binding by the cyanine dyes

The same experiments that were performed for the conjugates were also performed for the two free cyanine dyes (not conjugated to the DNA binding domains). Because the behavior of the two dyes used in this work was found to be essentially the same, the thermodynamic constants determined for the two cyanine dyes were averaged together and given as a single set of thermodynamic parameters. Table 3 summarizes the equilibrium constants (K_{obs}) and the corresponding binding free energies (ΔG^0) as a function of salt concentration (0.15–0.25 M Na^+) and temperature (275–313 K) determined by total fluorescence counts from the intercalating dyes as a function of dsDNA concentration. For these measurements, the dye concentration in each case was held constant at 50 nM, and the concentration of the nonspecific dsDNA fragment (see Fig. 2 for sequence) was varied between 5 nM and 50 μM. The equilibrium constants presented in Table 3 are given in terms of the number of moles of nonspecific dsDNA fragment that is the same length in base pairs as the two dsDNA fragments used above (HixL and TC3) containing specific binding sites. Note that similar experiments using the HixL or TC3

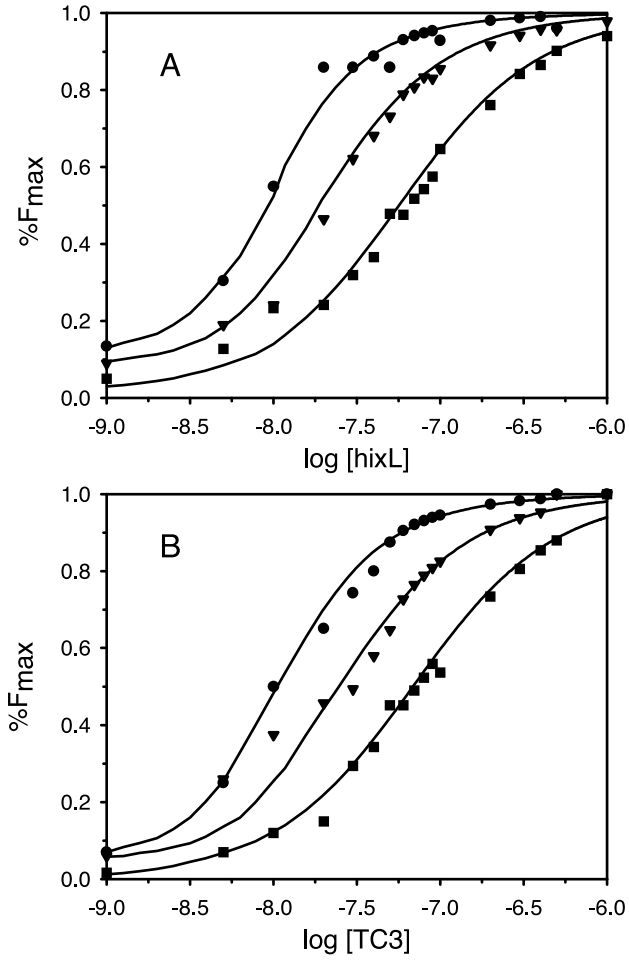

FIGURE 4 Representative binding curves the conjugates (*A*) YOHin and (*B*) TOTc3 binding to their respective unlabeled consensus DNA sequences (Fig. 2). The total fluorescence of 1 nM conjugate is plotted as a function of the log of the concentration of DNA. The solid lines represent fits to a theoretical binding curve. The titrations were performed as a function of salt concentration and temperature: ●, 298 K, 0.150 M Na^+; ▼, 313 K, 0.150 M Na^+; and ■, 298 K, 0.250 M Na^+.

dsDNA fragments gave essentially the same results for both the magnitudes and the salt and temperature dependences of the equilibrium constants. Binding of oxazole yellow or thiazole orange to calf thymus DNA also gives very similar results when the size of the DNA fragment is accounted for.

In the salt range examined here, the equilibrium constant for dye binding decreases less than twofold when the salt concentration is increased from 0.15 to 0.25 M salt (Table 3). These dyes exhibit a considerably lower dependence upon salt concentration than is observed for the whole conjugate (Table 2). This is most likely a function of the delocalized positive charge present on the cyanine dyes. The temperature dependence of the equilibrium binding constants for the unconjugated dyes is even weaker (Table 3).

TABLE 2 The equilibrium constants (K_{obs}) and binding free energies determined for sequence specific binding of YOHin and TOTc3 conjugates to their respective consensus DNA sequences

	YOHin conjugate			TOTc3 conjugate		
Temp (K)	[Na^+] (M)	K_{obs} (M^{-1}) $\times 10^{-6}$	ΔG° (kcal/mol)	[Na^+] (M)	K_{obs} (M^{-1}) $\times 10^{-6}$	ΔG° (kcal/mol)
275	0.150	22	−9.2	0.150	22	−9.2
278	0.150	21	−9.3	0.150	26	−9.4
283	0.150	40	−9.8	0.150	40	−9.8
288	0.150	61	−10.3	0.150	21	−9.6
293	0.150	143	−10.9	0.150	66	−10.5
298	0.150	83	−10.8	0.150	245	−11.4
303	0.150	60	−10.8	0.150	49	−10.7
308	0.150	41	−10.7	0.150	22	−10.4
313	0.150	29	−10.7	0.150	22	−10.5
298	0.175	67	−10.7	0.175	83	−10.8
298	0.200	37	−10.3	0.200	40	−10.4
298	0.225	29	−10.2	0.225	26	−10.1
298	0.250	14	−9.8	0.250	17	−9.9

Nonspecific binding of unconjugated peptides and conjugates

The salt and temperature dependence of nonspecific binding between Tc3 or Hin domains and DNA is shown in Figs. 5 and 6. The equilibrium constant is lower for nonspecific binding compared to specific binding for all samples and conditions. The site size (n), determined by the McGhee–von Hippel model, was roughly 9.8 for the DBDs alone and 10.6 for the conjugates, although this difference is approximately equivalent to the range of n values determined for both. At the highest salt concentration, the DBDs without the conjugated dyes bind the nonspecific sequence with an affinity approximately 50-fold lower than they bind to the appropriate consensus sequence (Fig. 5 *A*). At the same salt concentration, the peptide/dye conjugates bind to nonspe-

TABLE 3 The equilibrium constants (K_{obs}) determined for cyanine dye interaction with nonspecific DNA

Temp (K)	[Na^+] (M)	K_{obs} (M^{-1}) $\times 10^{-6}$	ΔG° (kcal/mol)
275	0.150	0.59	−7.3
278	0.150	0.61	−7.4
283	0.150	0.60	−7.5
288	0.150	0.64	−7.6
293	0.150	0.63	−7.8
298	0.150	0.63	−7.9
303	0.150	0.55	−8.0
308	0.150	0.54	−8.1
313	0.150	0.50	−8.2
298	0.175	0.56	−7.2
298	0.200	0.50	−7.2
298	0.225	0.48	−7.2
298	0.250	0.38	−7.0

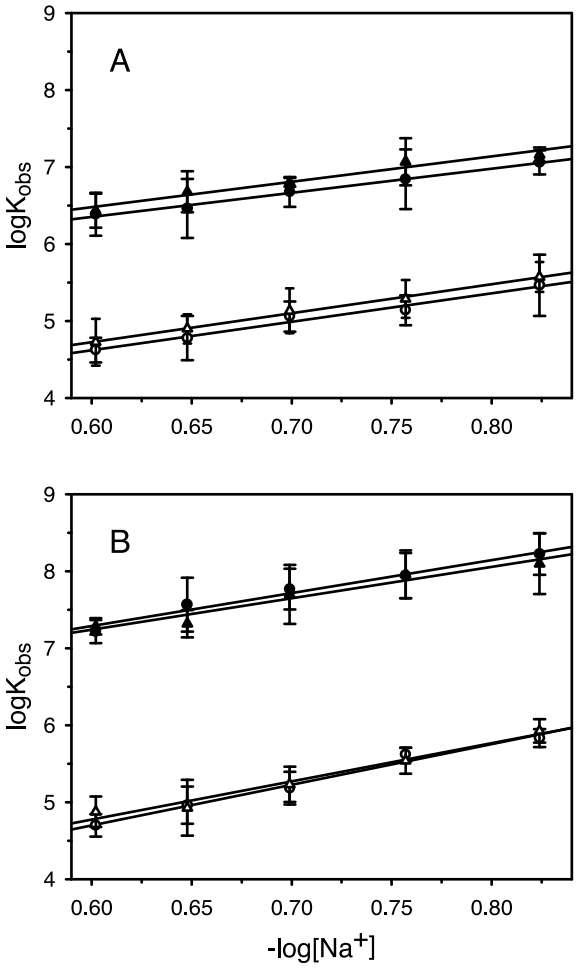

FIGURE 5 Dependence of log K_{obs} on $-\log[Na^+]$ for specific and nonspecific DNA-binding. (*A*) The salt dependence of the binding constants for the DNA-binding domains Hin (●) and Tc3 (▲) is shown for specific (*filled symbols*) and nonspecific (*open symbols*) binding. (*B*) The salt dependence of the conjugates YOHin (●) and TOTc3 (▲) is shown for specific (*filled symbols*) and nonspecific (*open symbols*) binding. Lines shown for each data set are calculated from Eq. 3.

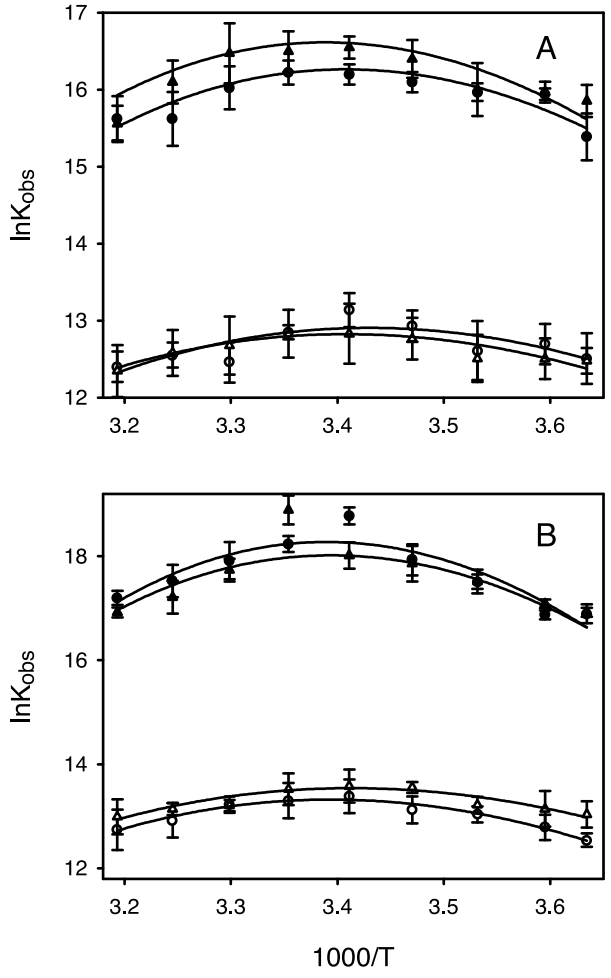

FIGURE 6 Dependence of ln K_{obs} on $1/T$ for specific and nonspecific DNA-binding. (*A*) The temperature dependence of the binding constants for the DNA-binding domains Hin (●) and Tc3 (▲) is shown for specific (*filled symbols*) and nonspecific (*open symbols*) binding. (*B*) The temperature dependence of the conjugates YOHin (●) and TOTc3 (▲) is shown for specific (*filled symbols*) and nonspecific (*open symbols*) binding. The solid lines represent a fit of the data to Eq. 4.

cific sequences with a 210- and 320-fold lower association constant for TOTc3 and YOHin, respectively, compared to the specific sequences (Fig. 5 *B*) For comparison, at the lowest salt concentration, the peptide/dye conjugates bind to nonspecific sequences with a 140- and 230-fold lower association constant for TOTc3 and YOHin, respectively (Fig. 5 *B*). Thus, as salt concentration is increased, nonspecific binding interactions between the protein and the DNA compete less effectively with binding of ions in solution and therefore the ratio of the nonspecific to specific equilibrium constants (K_{NS}/K_S) increases. This gives rise to the greater salt dependence observed for the nonspecifically bound complexes.

Although nonspecific interactions show a slightly greater dependence on salt than do specific interactions, the temperature dependence of nonspecific binding is weaker than that observed for specific binding. This is evident when comparing the data as a function of temperature for specific binding of each of the DNA-binding domains and their dye-labeled conjugates with the nonspecific binding by these same samples (Fig. 6). As the temperature is increased from 275 to 303 K, the specific interactions show a three- and ninefold increase in the association constants for the unconjugated (Fig. 6 *A*) and the conjugated (Fig. 6 *B*) DBDs, respectively. The nonspecific binding shows approximately a twofold increase in the association constant for both the conjugated and the unconjugated DBDs, again comparing 275 and 303 K. This greater dependence on temperature of specific binding is indicative of a larger negative change in heat capacity (described below).

DISCUSSION

The objective of these studies is to investigate the thermodynamic parameters of the sequence-specific and nonspecific DNA-binding by two native DBDs with and without a conjugated intercalating dye. The two HTH motifs used here are derived from the Hin recombinase and Tc3 transposase DNA-binding domains. The cyanine dyes are linked covalently to the ϵ-amine group of a lysine added to the N-terminal end of each of the DNA-binding domains. Both DBDs have a short N-terminal stretch of amino acids that is designed to place the dye into the minor groove of the DNA. The sequence recognition properties of the DBDs and conjugates were studied by steady-state fluorescence assays as a function of temperature and salt concentration. The DBDs and dye–DBD conjugates bind their cognate sequences with high affinity, having equilibrium constants in the range of 10^7 (DBDs) and 10^9 (conjugates).

Here, we have confirmed previous work from this lab, which indicated that the intercalating dye lends nonspecific binding affinity to the DBD when bound to its cognate site. Apparently, the DNA-binding domain is sufficient to confer sequence specificity, but requires other structural features of the protein, or, in this case, the additional stabilization by the intercalated dye, to maintain high binding affinity. These conjugates have the effect of reproducing binding affinity comparable to that of the complete native protein. The dye molecule augments the nonspecific binding affinity, often conferred by regions of the native protein that are not within the DNA-binding domain, while maintaining the specificity of the native protein. This will provide a useful framework for the engineering of site-specific DNA-interacting proteins and probes that are based on these binding domains.

In addition, we have determined the relevant thermodynamic parameters associated with the binding of both the Hin and Tc3 (with and without a conjugated dye). These two domains have been previously characterized structurally, but thermodynamic binding studies of these DBDs have not been previously performed.

Comparison of the polyelectrolyte effect for specific and nonspecific binding

Equilibrium constants for specific and nonspecific interactions are strong functions of the salt concentration. Ionic effects on K_{obs} have been modeled at a thermodynamic level in terms of the direct stoichiometric participation of ions in the protein–DNA association reaction (Record et al., 1976, 1978, 1991). A decrease in the equilibrium association constant with increasing ionic strength has been observed for a range of different cationic ligand–DNA interactions and is attributed to the competition between the positively charged ligands and the Na^+ ions for available DNA binding sites. In a solution of univalent salt, such as NaCl, at constant temperature, the stoichiometric representation of the association reaction of the probe (P) with a specific or nonspecific DNA site is

$$P a(Cl^-) + \text{DNA site } (b Na^+) \leftrightarrow \text{P-DNA complex} + a Cl^- + b Na^+.$$

Here, P-DNA represents the bound complex between the probe and the available DNA binding site. The apparent stoichiometric coefficients a and b are related to ions interacting with regions of the probe and DNA-binding site, respectively. Typically, $b \gg a$ because the DNA is a rod-like polyanion with a high axial charge density, whereas the region of the protein at the interface of the DNA is locally an oligoelectrolytic portion of the polyampholytic protein (Olmsted et al., 1989). The number of anions released is relatively negligible to a first approximation from oligoelectrolyte theory (Mascotti and Lohman, 1990; Olmsted et al., 1989), although a rigorous determination using different anions was not performed here. The dependence of the observed equilibrium constant on $[Na^+]$, results from the release of counterions (b) from the DNA in the association reaction with the DNA-binding domain or conjugate probe. From the polyelectrolyte theory (Manning, 1969, 1972), simple monovalent cations, like Na^+ and K^+, interact with a polyelectrolyte by direct condensation of counterions onto the polyion to reduce the axial charge density. The remaining charges on the polyelectrolyte are screened from each other by mobile counter- and co-ions of the bulk solution. The sum of the direct condensation of the counterions and the associated Debye–Huckel-type screening process neutralizes the high charge density along the DNA duplex due to the negatively charged phosphate groups, and stabilizes the duplex conformation. The number of counterions confined at any time due to direct or indirect interactions with each charge on the DNA is less than one and given by an empirical factor ψ. In typical B-form DNA, ψ equals 0.88 (Mascotti and Lohman, 1990). The distribution of positively and negatively charged side chains in the DNA bound form of the peptides and conjugates make their coulombic interactions with phosphate groups somewhat complicated. However, the salt concentration-dependent characteristics of K_{obs} for peptide and conjugate binding appears comparable to that of a simple oligocation (deHaseth et al., 1977).

For oligonucleotides of the length used here, (40 base pairs) the DNA behaves as a polyelectrolyte in the central region containing the cognate sites with a relatively homogeneous electric field perpendicular to the helical axis. In the absence of Mg^{2+} or other competitive ions, plots of $\log K_{obs}$ are a linear function of $-\log[Na^+]$ with a slope that is proportional to the number of ions displaced from DNA

phosphate groups and basic groups of the protein (deHaseth et al., 1977). It was determined that

$$\frac{\partial \log K_{obs}}{\partial[M^+]} = m'\psi, \quad (3)$$

where the bound form of the protein makes m' ion pairs with the DNA upon binding and $[M^+]$ is the molar concentration of the counterion, in this case, Na^+ (Record et al., 1976). Fits of the salt dependence of the equilibrium constants to Eq. 3 are shown in Fig. 5 and have fitting errors within 15%.

Analysis of the slope ($m'\psi$) in the fits of Fig. 5 yields that the number of cations displaced upon complex formation is ~3.5 for Hin and 3.7 for Tc3 (without conjugated dye). This is in good agreement with crystal structure data, which shows four salt bridges for sequence-specific binding of both the Tc3 and Hin domains.

In contrast to the unconjugated binding domains, the linear slopes of the sequence-specific binding interactions for the conjugated binding domains give 4.9 displaced ions for YOHin and 4.7 for TOTc3, (Fig. 5). These values are 1.4 and 1.0 cations larger, respectively, than those observed for the unconjugated binding domains. To further understand this, the same analysis of the polyelectrolyte effect for the cyanine dyes alone was performed. The cyanine dye has a single delocalized positive charge. The slope of the salt-dependence plot for the cyanine dye corresponds to 0.9 ions displaced upon dye intercalation (data not shown). The number of ions displaced for the DBD and the dye effectively add up to the number of ions displaced by the conjugate. Further examination of the free energy differences between each respective conjugate and DBD show a much smaller difference than would be observed if the thermodynamic contributions of the intercalating dye were solely an additive process. This strongly suggests that, in the conjugate–DNA interaction, there is considerable steric constraints or, as predicted previously (Thompson and Woodbury, 2000b), the unwinding of the DNA upon dye intercalation adversely affects some of the DNA–DBD contacts.

This analysis was extended to nonspecific DNA binding of the DBDs and their respective conjugates. Comparison of the slopes of the $\log K_{obs}$ versus $-\log$[salt] plots for both the Hin and Tc3 DBDs show a greater [salt] dependence for nonspecific binding than for specific binding. This phenomenon is commonly observed in sequence-specific DNA-binding proteins (Eriksson and Nilsson, 1995; Frank et al., 1997; Lundback et al., 1993; Oda et al., 1998). The salt dependence of the DNA-binding domains (without conjugated dye) show a release of an additional 0.3 and 0.7 ions for interaction of a nonspecific sequence with Tc3 and Hin, respectively, compared to specific binding (Table 4). For the conjugates, nonspecific binding results in the release of an additional 1.0 and 1.1 ions when TOTc3 and YOHin bind, respectively, compared to specific binding (Table 4). In general, nonspecific interactions are stabilized by the formation of the contact ion pairs between the phosphate groups of the DNA backbone and the basic amino acid side chains of the protein, as shown by previous salt-dependence studies (Edsall and McKenzie, 1978). The difference between the number of ions released when binding to specific versus nonspecific DNA sequences suggests that the Hin DBD, more so than the Tc3, uses these ion pairs as part of the sequence-recognition mechanism. This further supports the idea of a greater hydrophobic effect related to specific binding of these complexes to DNA, likely due to the reduction of the water-accessible nonpolar surface area (see for example, Livingstone et al., 1991).

TABLE 4 The effects of sequence specificity and dye labeling on the change in heat capacity and number of ions displaced upon association of Hin and Tc3 DBDs

	Specific		Non-specific	
	ΔC_p (kcal/K mol)	ions	ΔC_p (kcal/K mol)	ions
Hin recombinase				
Unconjugated	−0.69	3.5	−0.46	4.2
Conjugated	−1.14	4.9	−0.65	6.0
Tc3 transposase				
Unconjugated	−0.77	3.7	−0.42	4.0
Conjugated	−1.06	4.7	−0.55	5.7

Comparison of the hydrophobic effect for specific and nonspecific binding

It has been known for several decades that large negative changes in heat capacity are characteristic of protein folding and conformational changes (Privalov and Gill, 1988; Record et al., 1991). More recently, it has been shown that such changes in heat capacity are a feature common to protein–DNA interactions (Brenowitz et al., 1990; Jin et al., 1993; Ladbury et al., 1994; Merabet and Ackers, 1995; Takeda et al., 1992). The temperature dependence of K_{obs} (Figs. 5 and 6 and Tables 1–3) was fit to Eq. 4 to determine the standard heat capacity change, ΔC_p, for complex formation between specific and nonspecific dsDNA fragments and each DNA binding domain, domain/dye conjugate and unconjugated dye:

$$2.303 \times \log K_{calc} = 2.303 \times \log K_{obs} - \frac{\Delta H^o_{obs}}{R}\left(\frac{1}{T_i} - \frac{1}{T^*}\right) + \frac{\Delta C^0_p}{R}\left[\left(2.303 \times \log\frac{T_i}{T^*}\right) + \frac{T^*}{T_1} - 1\right]. \quad (4)$$

Here, $2.303 \times \log K_{obs}$ and ΔH^0_{obs} are values at $T^* = 298$ K. The choice of reference temperature (T^*) is arbitrary and

does not affect the results of the fit. The errors from fitting the equilibrium constants for each temperature to Eq. 4 are within 20% of the stated values for ΔC_p (Table 4). Eq. 4 (Frank et al., 1997) assumes that ΔC_p is independent of temperature within experimental uncertainty. It has been suggested (Baldwin, 1986; Ha et al., 1989) that the thermodynamics of processes, where ΔC_p is large and temperature independent, can be completely characterized by the heat capacity (ΔC_p) and two temperatures, T_H (the temperature at which $\Delta H^0 = 0$ and occurs at the maxima of the van't Hoff plot) and T_S (the temperature at which $\Delta S^0 = 0$ and occurs at the minima of a plot of ΔG^0 versus temperature). Using this approach, the changes in enthalpy and entropy upon binding as a function of temperature are given as

$$\Delta H^0 = \Delta C_p(T - T_H), \tag{5}$$

$$\Delta S^0 = \Delta C_p \times 2.303 \times \log\left(\frac{T}{T_s}\right). \tag{6}$$

Association constants for site-specific protein–DNA interactions typically exhibit maxima at temperatures in the physiological range (Revzin, 1990; deHaseth et al., 1977). This is observed, for example, in Fig. 6 *A*, which plots the $\ln K_{obs}$ as a function of $1/T$ for the unlabeled DBDs. The logarithm of the equilibrium constant shows a maximum at ~293 K for Hin and ~294 K for Tc3. Analysis of these data using Eq. 4 reveals a negative heat capacity change upon association for both the Hin ($\Delta C_p = -0.69$ kcal/K·mol) and Tc3 ($\Delta C_p = -0.77$ kcal/K·mol) domains. This is a common feature observed for sequence-specific protein–DNA interactions (Spolar and Record, 1994). The temperature dependence of the enthalpic and entropic contributions to the binding free energy can be evaluated using Eqs. 5 and 6. At 298 K, binding is both enthalpically and entropically favorable for both Hin ($\Delta H^0 = -2.8$ kcal/mol and $\Delta S^0 = 16$ cal/K·mol) and Tc3 ($\Delta H^0 = -3.0$ kcal/mol and $\Delta S^0 = 23$ cal/K·mol). Sequence-specific binding for both nonlabeled DNA-binding domains become enthalpically favorable and entropically unfavorable as temperature increases, such that, at 313 K, association is entirely enthalpically driven for the Hin ($\Delta H^\circ = -13.1$ kcal/mol and $\Delta S^0 = -19$ cal/K·mol) and Tc3 ($\Delta H^0 = -14.6$ kcal/mol and $\Delta S^0 = -16$ cal/K·mol) alike.

A similar dependence on temperature for site-specific protein–DNA interactions is also observed for both conjugates (Fig. 6 *B*). Analysis of these data reveal a negative heat capacity change upon association ($\Delta C_p = -1.14$ kcal/K·mol) for YOHin and ($\Delta C_p = -1.06$ kcal/K·mol) for TOTc3. The changes in heat capacity are larger for the conjugates than for the unconjugated peptides binding to the same site, due to the predominantly hydrophobic surface area of the cyanine dye. As was the case for the unconjugated DNA-binding domains, at 298 K, binding is both enthalpically and entropically favorable for the TOTc3 ($\Delta H = -3.8$ kcal/mol and $\Delta S = 20$ cal/K·mol), and the YOHin ($\Delta H = -3.7$ kcal/mol and $\Delta S = 19$ cal/K·mol) when bound to the cognate sequence (Fig. 7).

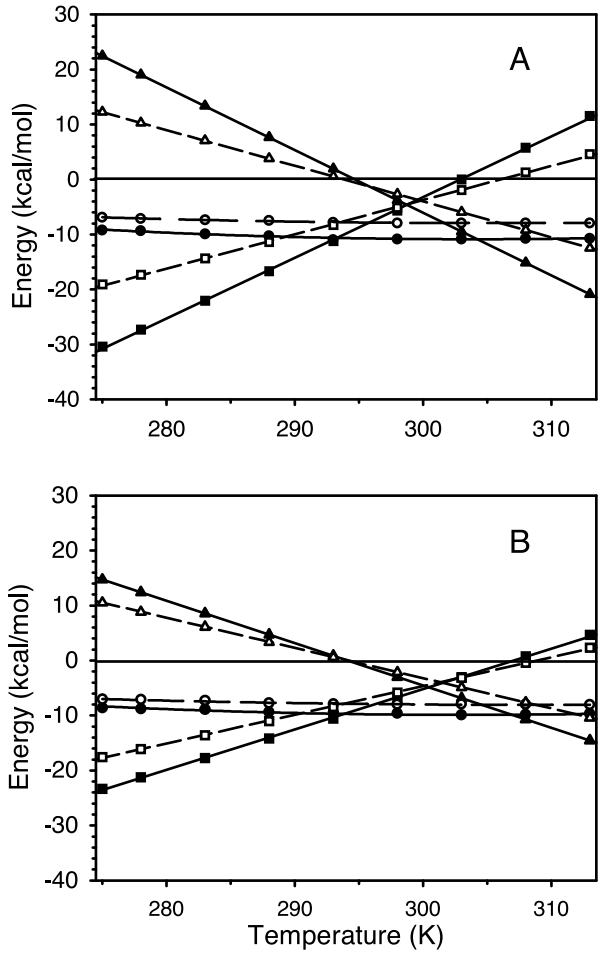

FIGURE 7 Thermodynamic profiles of the DNA-binding reaction of the (*A*) YOHin and (*B*) TOTc3 conjugate for specific (*filled symbols*) and nonspecific (*open symbols*) binding as determined by total fluorescence. Plot of the free energy (●), enthalpy (▲), and entropy (■) of binding versus temperature. It should be noted that the entropy is given as $-T\Delta S$ to present the data with enthalpy and free energy in the same units. Experimental errors for the determination of the thermodynamic parameters are in the range of 10 to 40%.

Similar analysis of the temperature dependence of K_{obs} for the cyanine dyes alone reveals a moderate negative heat capacity change upon association ($\Delta C_p = -0.15$ kcal/K·mol, Tables 3 and 4). The changes in heat capacity are smaller for the dyes alone than for either the unconjugated peptides or the conjugates. The change in the heat capacity for the dyes alone is close to that determined for the intercalators ethidium bromide ($\Delta C_p = -0.14$ kcal/K·mol) and propidium iodide ($\Delta C_p = -0.15$ kcal/K·mol), which demonstrated that the overwhelming driving force is derived from the hydrophobic effect (Ren et al., 2000).

A clear trend in the thermodynamic parameters exists between the binding of the consensus sequence versus the nonspecific sequence across all the species studied here. In

terms of the hydrophobic effect, the magnitude of the negative change in the heat capacity (ΔC_p) is larger for the specifically bound complexes than for nonspecific binding (Table 4). This can be seen in Fig. 6, where the extent of the curvature in the van't Hoff plots is reduced in going from specific to nonspecific for both the DNA-binding domains (Fig. 6 *A*) and the conjugates (Fig. 6 *B*). The smaller negative change in heat capacity for binding to nonspecific sequences is typically attributed to a larger dehydrated surface area at the protein–DNA interface for the cognate sequence than for the nonspecific sequence. For the nonspecific sequence, the interface is more hydrated and less complementary.

Several comparisons can be made from the differences in the heat capacity changes summarized in Table 4 as they relate to differences in water-exposed hydrophobic surface areas for each complex. First, a comparison of the heat capacity change for specific and nonspecific complexes for the DBDs yields information about the differences in the binding interface and induced structural changes upon complex formation. Next, a comparison of the specifically bound DBD with its respective conjugate yields information about how the attached dye affects the bound complex. In the case of the unconjugated DBDs, the Hin and Tc3 complexes show a ΔC_p difference between the specific and nonspecific complexes of 0.23 and 0.35, respectively. As described above, the bulk of this difference in each case is likely a result of the larger solvent-exposed surface area in the nonspecific complex, which does not form a tight fit at the macromolecular interface, compared to the specifically bound complex. The larger change in ΔC_p between specific and nonspecific sequences for Tc3 versus the Hin may arise from more significant ordering or conformational changes upon binding of Tc3 versus Hin. Ordering of regions of the peptide upon binding should affect the heat capacity changes. Preliminary circular dichroism measurements from our lab show that the Hin peptide does not show a significant structural change upon interaction with its consensus site, whereas the Tc3 shows an enhanced signal at 222 nm upon complex formation (unpublished results).

The conjugation of the dye to each DBD shows a greater increase in the ΔC_p than can be attributed to the cumulative effects of the dye itself (the dye itself shows $\Delta C_p = -0.15$ kcal/K·mol). The increase in the ΔC_p is 0.45 for the YOHin and 0.29 for the TOTc3 comparing conjugated and unconjugated binding domains. Here, the relationship between the change in heat capacity and solvent-exposed surface area suggest that the conjugated dye exerts an effect on the structure of the bound complexes that is greater than simply the additional change in heat capacity provided by the dye. In the specifically bound complex of Hin with the hixL consensus site, the short stretch of amino acids that resides in the minor groove is likely disordered and has a great deal of mobility in solution. Crystal structure data (Feng et al., 1994) and a molecular dynamic simulation (Robinson and Sligar, 1996) of the Hin–hixL complex both indicate the N-terminal arm of the Hin is quite mobile in solution. This region may be forced to spend more time in the minor groove when the dye is conjugated to the peptide. Here, the intercalated dye can act as an anchor–further stabilizing the binding in this region and possibly slowing the dissociation kinetics of this portion of the DNA-binding domain. The dye attached to the Tc3 may affect the bound complex in the same way to some extent. However, in the Tc3, the stretch of N-terminal amino acids in the minor groove is shorter than for the Hin and is highly ordered in the crystal structure of the DNA-bound Tc3 complex (van Pouderoyen et al., 1997). Thus, the dye may play less of an anchoring role in the Tc3 complex.

This work was supported in part by a grant from the US department of Agriculture (98-35306-6396).

REFERENCES

Baldwin, R. L. 1986. Temperature-dependence of the hydrophobic interaction in protein folding. *Proc. Natl. Acad. Sci. U.S.A.* 83:8069–8072.

Bourdouxhe, C., P. Colson, C. Houssier, J. S. Sun, and T. Montenay-Garestier. 1992. Binding of a distamycin-ellipticene hybrid molecule to DNA and chromatin: spectroscopic, biochemical and molecular modelling investigations. *Biochemistry.* 31:12385–12396.

Brenowitz, M., E. Jamison, A. Majumdar, and S. Adhya. 1990. Interaction of the *Escherichia coli* gal repressor protein with its DNA operators in vitro. *Biochemistry.* 29:3374–3383.

Brown, C. L., and M. M. Harding. 1994. Synthetic alpha-helical peptides incorporating intercalators for DNA recognition. *J. Mol. Recognit.* 7:215–220.

Bruist, M. F., S. J. Horvath, L. E. Hood, T. A. Steitz, and M. I. Simon. 1987. Synthesis of a site-specific DNA-binding peptide. *Science.* 235:777–780.

Bulsink, H., B. Harmsen, and C. Hilbers. 1985. Specificity of the binding of bacteriophage-M13 encoded gene-5 protein to DNA and RNA studied by means of fluorescence titrations. *J. Biomol. Struct. Dyn.* 3:227–247.

Cantor, C. R., and P. R. Schimmel. 1980. The Conformation of Biological Macromolecules. W.H. Freeman, San Francisco. 377.

Caruthers, M. H., A. D. Barone, S. L. Beaucage, D. R. Dodds, E. F. Fisher, L. J. McBride, M. Matteucci, Z. Stabinsky, and J. Y. Tang. 1987. Chemical synthesis of deoxyoligonucleotides by the phosphoramidite method. *Methods Enzymol.* 154:287–313.

Daniel, D. C., M. Thompson, and N. W. Woodbury. 2000. Fluorescence intensity fluctuations of individual labeled DNA fragments and a DNA binding protein in solution at the single molecule level: a comparison of photobleaching, diffusion, and binding dynamics. *J. Phys. Chem.* 104: 1382–1390.

deHaseth, P. L., T. M. Lohman, and M. T. Record. 1977. Nonspecific interaction of lac repressor with DNA: association reaction driven by counterion release. *Biochemistry.* 16:4783–4790.

Dervan, P. B., J. S. Taylor, and P. G. Schultz. 1984. DNA affinity cleaving. *Tetrahedron.* 40:457–465.

Dwyer, T. J., B. H. Geierstanger, Y. Bathini, J. W. Lown, and D. E. Wemmer. 1992. Design and binding of a distamycin analog to d(CG-CAAGTTGGA)- d(GCCAACTTGCG): synthesis, NMR studies, and implications for the design of sequence-specific minor groove binding oligopeptides. *J. Am. Chem. Soc.* 114:5911–5919.

Edsall, J. T., and H. A. McKenzie. 1978. Water and proteins. The location and dynamics of water in protein systems and its relation to their stability and properties. *Adv. Biophys.* 10:137–207.

Eriksson, M. A. L., and L. Nilsson. 1995. Structure, thermodynamics and cooperativity of the glucocorticoid receptor DNA-binding domain in

complex with different response elements. Molecular dynamics simulation and free energy perturbation studies. *J. Mol. Biol.* 253:453–472.

Feng, J.-A., R. C. Johnson, and R. E. Dickerson. 1994. Hin recombinase bound to DNA: the origin of specificity in major and minor groove interactions. *Science.* 263:348–355.

Frank, D. E., R. M. Saeker, J. P. Bond, M. W. Capp, O. V. Tsodikov, S. E. Melcher, M. M. Levandoski, and M. T. Record. 1997. Thermodynamics of the interactions of lac repressor with variants of the symmetric lac operator: effects of converting a consensus site to a non-specific site. *J. Mol. Biol.* 267:1186–1206.

Fritsch, E. F., and T. Maniatis. 1989. Molecular Cloning: A Laboratory Manual. Cold Spring Harbor Laboratory, Cold Spring Harbor, NY. 11–46.

Ha, J.-H., R. S. Spolar, and M. T. Record. 1989. Role of the hydrophobic effect in stability of site-specific protein-DNA complexes. *J. Mol. Biol.* 209:801–816.

Haugland, R. P. 1996. Handbook of Fluorescent Probes and Research Chemicals. Molecular Probes, Inc., Eugene, OR. 144–156.

Hughes, K. T., P. C. W. Gaines, J. E. Karlinsey, R. Vinayak, and M. I. Simon. 1992. Sequence specific interaction of the Salmonella Hin recombinase in both major and minor grooves of DNA. *EMBO J.* 11: 2695–2705.

Jin, L., J. Yang, and J. Carey. 1993. Thermodynamics of ligand binding to trp repressor. *Biochemistry.* 32:7302–7309.

Kendrew, J. C., and E. Lawrence. 1994. The Encyclopedia of Molecular Biology. *In* Hybridization. Oxford University Press, Cambridge, UK. 503–506.

Kent, S. B. H. 1988. Chemical synthesis of peptide and proteins. *Annu. Rev. Biochem.* 57:957–989.

Ladbury, J. E., J. G. Wright, J. M. Sturtevant, and P. B. Stigler. 1994. A thermodynamic study of the Trp repressor–operator interaction. *J. Mol. Biol.* 238:669–681.

Lampe, D., M. Churchill, and H. Robertson. 1996. A purified mariner transposase is sufficient to mediate transposition in vitro. *EMBO J.* 15:5470–5479.

Latchman, D. S. 1990. Eukaryotic transcription factors. *Biochem. J.* 270: 281–289.

Livingstone, J. R., R. S. Spolar, and M. T. Record. 1991. Contribution to the thermodynamics of protein folding from the reduction in water-accessible nonpolar surface-area. *Biochemistry.* 30:4237–4244.

Lundbäck, T., C. Cairns, J.-A. Gustafsson, J. Carlstedt-Duke, and T. Hard. 1993. Thermodynamics of the glucocorticoid receptor–DNA interaction: binding of wild type GR DBD to different response elements. *Biochemistry.* 32:5074–5082.

Mack, D. P., and P. B. Dervan. 1990. Nickel mediated sequence specific oxidative cleavage of DNA by a designed metalloprotein. *J. Am. Chem. Soc.* 112:4604–4606.

Manning, G. S. 1969. Limiting laws and counterion condensation in polyelectrolyte solutions. I. Colligative properties. *J. Chem. Phys.* 51: 924–933.

Manning, G. S. 1972. On the application of polyelectrolyte "limiting laws" to the helix-coil transition of DNA. I. Excess univalent cations. *Biopolymers.* 11:937–949.

Mascotti, D., and T. Lohman. 1990. Thermodynamic extent of counterion release upon binding oligolysines to single-stranded nucleic-acids. *Proc. Natl. Acad. Sci. U.S.A.* 87:3142–3147.

McGhee, J. D., and P. H. von Hippel. 1974. Theoretical aspects of DNA–protein interactions: cooperative and non-cooperative binding of large ligands to a one dimensional homogeneous lattice. *J. Mol. Biol.* 86:469–489.

Merabet, E., and G. K. Ackers. 1995. Calorimetric analysis of l cI repressor binding to DNA operator sites. *J. Mol. Biol.* 34:8554–8563.

Oda, M., K. Furukawa, K. Ogata, A. Sarai, and H. Nakamura. 1998. Thermodynamics of specific and non-specific DNA binding by the c-Myb DNA-binding domain. *J. Mol. Biol.* 276:571–590.

Olmsted, M., C. F. Anderson, and M. T. Record. 1989. Monte Carlo description of oligoelectrolyte properties of DNA oligomers: range of the end effect and the approach of molecular and thermodynamic properties to the polyelectrolyte limits. *Proc. Natl. Acad. Sci. U.S.A.* 86:7766–7770.

Pabo, C. O., and M. Lewis. 1982. The operator-binding domain of l-repressor: structure and DNA recognition. *Nature.* 298:443–447.

Pabo, C. O., and R. T. Sauer. 1992. Transcription factors: structural families and principles of DNA recognition. *Annu. Rev. Biochem.* 61: 1053–1095.

Plasterk, R. H. A. 1996. The Tc1/mariner transposon family. *Curr. Topics Microbiol. Immunol.* 204:125–143.

Privalov, P. L., and S. J. Gill. 1988. Stability of protein structure and hydrophobic interaction. *Adv. Protein Chem.* 39:191–234.

Record, M. T., T. M. Lohman, and P. deHaseth. 1976. Ion effects on ligand–nucleic acid interactions. *J. Mol. Biol.* 107:145–158.

Record, M. T., C. F. Anderson, and T. M. Lohman. 1978. Thermodynamic analysis of ion effects on the binding and conformational equilibria of proteins and nucleic acids: the roles of ion association or release, screening and ion effects on water activity. *Quart. Rev. Biophys.* 11: 102–178.

Record, M., J. Ha, and M. Fisher. 1991. Analysis of equilibrium and kinetic measurements to determine thermodynamic origins of stability and specificity and mechanism of formation of site specific complexes between proteins and helical DNA. *Methods Enzymol.* 208:291–343.

Ren, J., T. Jenkins, and J. Chaires. 2000. Energetics of DNA intercalation reactions. *Biochemistry.* 39:8439–8447.

Revzin, A. 1990. The Biology of Non-Specific DNA-Protein Interactions. CRC Press, Boca Raton, FL. 33–69.

Rye, H., S. Yue, D. Wemmer, M. Quesada, R. Haugland, R. Mathies, and A. Glazer. 1992. Stable fluorescent complexes of double-stranded DNA with bis-intercalating asymmetric cyanine dyes: properties and applications. *Nucl. Acids Res.* 20:2803–2812.

Robinson, C. R., and S. G. Sligar. 1996. Participation of water in Hin recombinase-DNA recognition. *Prot. Sci.* 5:2119–2124.

Sardesai, N. Y., and J. K. Barton. 1997. DNA recognition by metal–peptide complexes containing the recognition helix of the phage 434 repressor. *J. Biol. Inorg. Chem.* 2:762–771.

Shin, J. A., R. H. Ebright, and P. B. Dervan. 1991. Orientation of the lac repressor DNA binding domain in complex with the left lac operator half site characterized by affinity cleaving. *Nucl. Acids Res.* 19:5233–5236.

Sluka, J. P., S. J. Horvath, M. F. Bruist, M. I. Simon, and P. B. Dervan. 1987. Synthesis of a sequence specific DNA-cleaving peptide. *Science.* 238:1129–1132.

Spolar, R. S., and M. T. Record. 1994. Coupling of local folding to site-specific binding of proteins to DNA. *Science.* 362:777–784.

Takeda, Y., P. D. Ross, and C. P. Mudd. 1992. Thermodynamics of Cro protein–DNA interactions. *Proc. Natl. Acad. Sci. U.S.A.* 89:8180–8184.

Thompson, M. 2000. Synthesis and characterization of the photophysical and photochemical properties of sequence specific fluorescent DNA-binding probes. Ph.D. Dissertation, Arizona State University, Tempe, AZ. 164.

Thompson, M., and N. W. Woodbury. 2000a. Photophysical properties of a single zinc finger crosslinked with a fluorescent DNA-binding probe. *Biophys. J.* 78:300 (Abstr.).

Thompson, M., and N. W. Woodbury. 2000b. Fluorescent and photochemical properties of a single zinc finger conjugated to a fluorescent DNA-binding probe. *Biochemistry.* 39:4327–4338.

Tokuda, M., K. Fujiwara, T. Gomibuchi, M. Hirama, M. Uesugi, and Y. Sugiura. 1993. Synthesis of a hybrid molecule containing neocarzinostatin chromaphore analog and minor groove binder. *Tetrahedron Lett.* 34:669–672.

van Pouderoyen, G., R. F. Ketting, A. Perrakis, R. H. A. Plasterk, and T. K. Sixma. 1997. Crystal structure of the specific DNA-binding domain of Tc3 transposase of *C. elegans* in complex with transposon DNA. *EMBO J.* 16:6044–6054.

Vos, J. C., I. DeBaere, and R. H. A. Plasterk. 1996. Transposase is the only nematode protein required for in vitro transposition Tc1. *Genes Dev.* 10:755–761.